Isoform Specific Differences in Binding of a Dual-Specificity A-Kinase Anchoring Protein to Type I and Type II Regulatory Subunits of PKA†

Lora L. Burns,‡ Jaume M. Canaves,‡ Juniper K. Pennypacker,‡ Donald K. Blumenthal,§ and Susan S. Taylor*,‡

Howard Hughes Medical Institute, Department of Chemistry and Biochemistry, University of California, San Diego, 9500 Gilman Drive, La Jolla, California 92093-0654 and Departments of Pharmacology & Toxicology, and Biochemistry, University of Utah, 30 South 2000 E., Room 201, Salt Lake City, Utah 84112

Received August 5, 2002; Revised Manuscript Received March 19, 2003

ABSTRACT: Dual-specificity AKAPs bind to type I (RI) and type II (RII) regulatory subunits of cAMP-dependent protein kinase A (PKA), potentially recruiting distinct cAMP responsive holoenzymes to a given intracellular location. To understand the molecular basis for this "dual" functionality, we have examined the pH-dependence, the salt-dependence, and the kinetics of binding of the A-kinase binding (AKB) domain of D-AKAP2 to the regulatory subunit isoforms of PKA. Using fluorescence anisotropy, we have found that a 27-residue peptide corresponding to the AKB domain of D-AKAP2 bound 25-fold more tightly to RIIα than to RIα. The higher affinity for RIIα was the result of a slower off-rate as determined by surface plasmon resonance. The high-affinity interaction for RIα and RIIα was pH-independent from pH 7.4 to 5.0. At pH 4.0, both isoforms had a reduction in binding affinity. Additionally, binding of the AKB domain to RIα was independent of solution ionic strength, whereas RIIα had an increased binding affinity at higher ionic strength. This suggests that the relative energetic contribution of the charge stabilization is different for the two isoforms. This prediction was confirmed by mutagenesis in which acidic mutations, primarily of E10 and D23, in the AKB domain affected binding to RIα but not to RIIα. These isoform-specific differences provide a foundation for developing isoform-specific peptide inhibitors of PKA anchoring by dual-specificity AKAPs, which can be used to evaluate the physiological significance of dual-specificity modes of PKA anchoring.

Cyclic AMP-dependent protein kinase, also known as protein kinase A (PKA),[1] is the major receptor for the second messenger cAMP in eukaryotic cells. The PKA signaling pathway is activated through many different cell surface receptors, and once PKA is activated by cAMP binding, it phosphorylates numerous protein substrates involved in diverse biochemical processes such as metabolism, ion fluxes, cell migration, neuronal transmission, cell division, and gene transcription (*1*). A considerable amount of work over the past decade has focused on understanding how signal specificity is achieved for such a ubiquitous kinase.

PKA in its inactive state is a tetramer consisting of a regulatory subunit homodimer and two catalytic subunits (*1*). The regulatory subunit homodimer binds to the catalytic subunits and directly inhibits their catalytic activity. The homodimer also serves as a docking surface for A-kinase anchoring proteins (AKAPs) and indirectly controls activation and substrate specificity of the kinase through subcellular localization (*2*). AKAPs have been identified that target PKA to many different intracellular compartments (*3*). AKAPs also function as molecular scaffolds that bind other signaling proteins such as protein phosphatases and cyclic nucleotide diesterases thereby coordinating and integrating PKA signaling at the targeted site, lending specificity and a high degree of temporal and spatial control to the kinase. Interaction of the regulatory subunit with AKAPs is therefore integral in directing and regulating the response mediated by cAMP binding to PKA.

There are four regulatory subunit isoforms of PKA (RIα, RIβ, RIIα, RIIβ) (*4*). The domain structure of each isoform is similar with a dimerization/docking (D/D) domain at the N-terminus, two tandem cAMP-binding domains, and an interconnecting flexible hinge region, which contains the kinase pseudosubstrate inhibitory site. The D/D domain enables regulatory subunit dimerization and upon formation of a subunit dimer provides an interface for AKAP binding (*5*, *6*). The flexible pseudosubstrate inhibitor site provides a direct binding site for the catalytic subunit, inhibiting its activity in the absence of cAMP. The tandem, cAMP binding sites bind cAMP cooperatively and couple cAMP binding to catalytic subunit activation.

Despite similar domain structure, the regulatory subunit isoforms of PKA differ in tissue distribution, antigenicity,

† This work was funded by an NIH grant (DK-54441) to S.S.T. L.L.B. was funded by an NIH training grant (5T32 DK-07233).

* Corresponding author: Susan S. Taylor, Howard Hughes Medical Institute, University of California, San Diego, 9500 Gilman Drive, La Jolla, CA 92093-0654. Phone: (858) 534−3677. Fax: (858) 534−8193. E-mail: staylor@ucsd.edu.

‡ University of California.

§ University of Utah.

[1] Abbreviations: PKA, cAMP-dependent protein kinase; AKAP, A-kinase anchoring protein; D-AKAP, dual-specificity AKAP; RI and RII, type I and type II regulatory subunits, respectively; D/D domain, dimerization/docking domain of regulatory subunit; AKB domain, A-kinase binding domain; TCEP, tris-(2-carboxyethyl) phosphine hydrochloride; TFA, trifluoroacetate; CD, circular dichroism; SDS, sodium dodecyl sulfate; FFT, fast Fourier transform.

10.1021/bi0265729 CCC: $25.00
Published on Web 04/22/2003

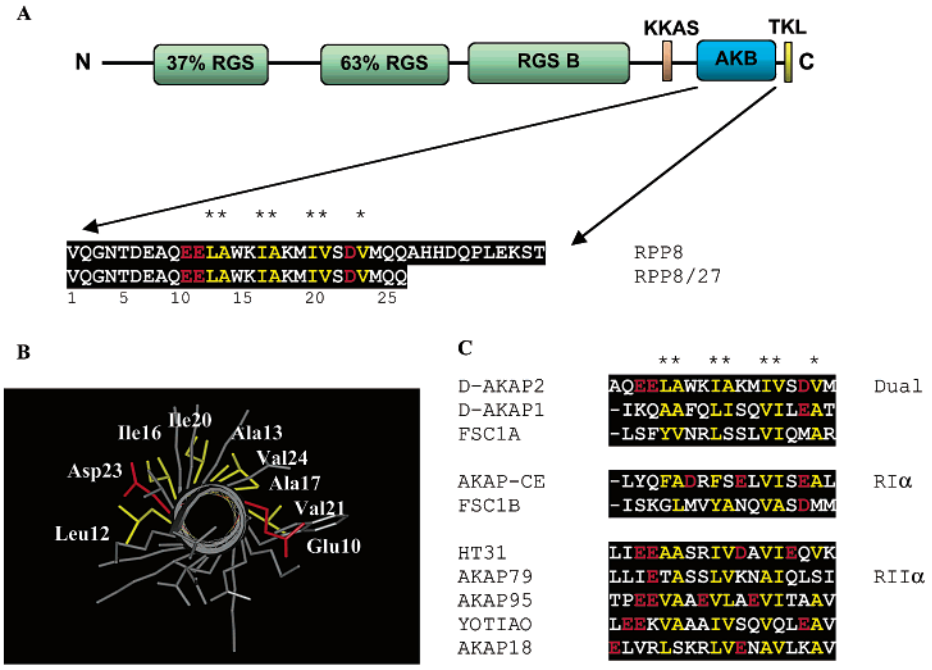

FIGURE 1: (A) The domain organization of full-length, human D-AKAP2 illustrating two regulators of G protein signaling (RGS) domains (one of which is separated by a 124-amino acid insert), a PKA phosphorylation site (KKAS), a protein kinase A binding (AKB) domain, and a PDZ binding motif (TKL-COOH). The sequence of RPP8 initially identified in a genomic screen as interacting with the regulatory subunit and the sequence corresponding to a smaller fragment (27 amino acids, RPP8/27) that is predicted to form an α-helix are indicated. (B) A helical wheel representation of the smaller fragment, RPP8/27, showing the amphipathic nature of the helix with hydrophobic groups highlighted in yellow on one face of the helix. The acidic residues that border each side of the hydrophobic binding surface are shown in red. Amino acid side chains are labeled. (C) An alignment of selected AKAPs that are dual-specificity, RIα-specific, and RIIα-specific. The conserved repeating units of hydrophobic residues (yellow), which are characteristic of this family of proteins, are highlighted. Acidic residues are in red. The alignment for the RII specific AKAPs: HT31, AKAP79, AKAP 95, Yotiao and AKAP18 is consistent with the alignment presented in Newlon et al. (*6*). (D-AKAP2, dual-specificity AKAP 2; D-AKAP1, dual-specificity AKAP 1; FSC1A, fibrin sheath component domain A; AKAP-CE, AKAP *C. elegans*; FSC1B, fibrin sheath component domain B; Ht31, human thyroid 31).

cAMP sensitivity, and AKAP-mediated localization (*4*, *7*). The type I isoforms are primarily distributed diffusely in the cytoplasm but can be recruited to specific intracellular sites such as the neuromuscular junction (*8*), the microtubules (*9*), and the cap site of lymphocytes upon antigen activation (*10*). The type II isoforms are generally localized to intracellular compartments and partition with the membrane soluble fraction. The alpha subtypes of each isoform are predominantly expressed in nearly all tissues, while the beta subtypes are enriched in selected tissues such as brain, adipocytes, and testes. Phenotypic studies using knock-out mice have shown that these isoforms have distinct functions (*11*). In RIIβ knockout mice, RIα expression is upregulated, but the mice have novel phenotypes (*12*, *13*). The mice are lean and have alterations in metabolism. The corresponding knockout of RIα results in embryonically lethal mice highlighting the essential nature of this isoform (*12*, *14*).

Historically, AKAPs were functionally identified by their ability to bind to the RII isoform. D-AKAP2 or AKAP10 was initially identified as interacting with the RIα subunit in a genomic screen and was subsequently shown to bind to RII (*15*). The discovery that some AKAPs (dual-specificity AKAPs, D-AKAPs) have the ability to bind to both the type I and type II isoforms of PKA suggests a role for these AKAPs in diversifying the cAMP-mediated signaling pathway.

We have previously reported on the domain organization of D-AKAP2 (*16*). D-AKAP2 contains two putative regulators of G protein signaling (RGS) domains, a protein kinase A binding (AKB) domain and a PDZ binding motif (Figure 1). The multidomain architecture of D-AKAP2 enables this protein to act as a scaffold, potentially coordinating upstream G protein signaling with downstream PKA signaling. In this report, we have further defined the AKB domain of D-AKAP2 and have examined the isoform specificity of binding of this domain to the regulatory subunit isoforms. We have found that a 27-residue peptide corresponding to the AKB domain is unstructured at pH 7.0 and undergoes a helix transition at low pH. The unstructured peptide binds in the nanomolar range to both type I and type II regulatory subunits and their corresponding dimerization/docking (D/D) domains. Given the amphipathic nature of the AKB domain sequence, this suggests helix induction of the AKAP peptide upon binding. We present the kinetics, the pH- and the salt-dependence of binding of the AKB domain to the regulatory subunit isoforms of PKA, and suggest isoform-specific differences in their interaction.

MATERIALS AND METHODS

Peptide Synthesis and Purification. A 27-residue peptide (RPP8/27) (VQGNTDEAQEELAWKIAKMIVSDVMQQ) corresponding to the PKA binding (AKB) domain of D-AKAP2 was synthesized by SynPep Corporation (Dublin, CA). A C-terminal Cys was added to enable fluorescence labeling and the C-terminus was carboxamide protected. The peptide was HPLC purified by SynPep and the mass verified by mass spectrometry with an average mass of 3164 atomic mass units, which is nearly identical to the expected mass

of 3164.6. The peptide was fluorescently labeled using a 25 mM solution of tetramethylrhodamine-5-maleimide (catalog number T-6027; Molecular Probes, Eugene, OR) dissolved in DMSO. The peptide was labeled by incubating it with a 3-fold molar excess of the label for 16 h at 4 °C in 20 mM Tris, pH 7.0 and 1 mM TCEP (nonthiol reducing agent, Molecular Probes). The sample was quenched with 1 mM β-mercaptoethanol to bind to any unreacted maleimide and diluted with 0.1% TFA for purification by HPLC. The labeled peptide was resolved using a C18 column with a water/acetonitrile gradient containing 0.1% TFA. The mass of the labeled peptide was verified by mass spectrometry and found to be 3645.95, which was consistent with a thioether-linked rhodamine label. The peptide concentration was determined by diluting into 100% methanol and using an extinction coefficient of 91000 M^{-1} cm^{-1} for absorbance of the rhodamine label at 541 nm (Molecular Probes Catalog). The peptide was stored at 4 °C in 50% acetonitrile.

Protein Expression and Purification. RPP8 (40 amino acids) was cloned into a thrombin-cleavable GST-tagged vector as previously described (*15*). The protein was purified using a glutathione resin in phosphate buffered saline (PBS). After elution of the sample from the resin, the GST tag was cleaved with thrombin and further purified using an S75-Sephadex (16/60) gel filtration column (Pharmacia). After thrombin cleavage, the sequence contained an additional 15 residues (GSPGISGGGGGILLS) at the N-terminus in addition to the 40 amino acids from D-AKAP2. The peptide was dialyzed in 50 mM ammonium bicarbonate and lyophilized. The peptide concentration was determined using an extinction coefficient of 0.96 mL mg^{-1} cm^{-1} at 280 nm based on the method of Pace et al. (*17*).

Murine RIIα and rat RIIβ were expressed in *Escherichia coli* BL21 (DE3). Bovine RIα was expressed in *E. coli* 222 cells. The proteins were purified as previously described using a cAMP affinity resin (*16*). The protein concentrations were determined using the following extinction coefficients at 280 nm, which were calculated using a standard concentration of protein calibrated using quantitative amino acid analysis: RIα 52603 M^{-1} cm^{-1}, RIIβ 42588 M^{-1} cm^{-1} and RIIα 62456 M^{-1} cm^{-1}. The proteins were stored at 4 °C in 50 mM MES, pH 5.8, 50 mM NaCl, 2 mM EDTA, 2 mM EGTA, 2 mM DTT.

Murine RIIα D/D (residues 1−44) was cloned into pET15b (Invitrogen), a His-tagged vector, using NdeI and BamHI. The protein was expressed in BL21(DE3) cells and purified using Talon resin (Clontech). The His-tag was cleaved from the protein and the protein further purified using an S75-Sephadex (16/60) gel filtration column (Pharmacia) in 50 mM sodium acetate, 200 mM NaCl, 2 mM EDTA pH 4.0. Bovine RIa D/D (residues 12−61) was purified as previously described (*18*, *19*). Extinction coefficients at 280 nm were based on the method of Pace et al. and were 5960 M^{-1} cm^{-1} and 6210 M^{-1} cm^{-1} for RIIα D/D and RIα D/D, respectively (*17*).

Circular Dichroism (CD) Spectroscopy. CD measurements were carried out on an AVIV 202 spectropolarimeter. Spectra were measured over the range of 180−260 nm using a 0.1 cm cell, 1 nm bandwidth, an averaging time of 4 s, and a cell temperature of 25 °C. CD spectra were obtained using 32 μM peptide over a range of pH values after 1 h equilibration. The following buffers were used: pH 7.5−pH 6.0, 50 mM sodium phosphate buffer, pH 5.0−pH 3.0, 50 mM sodium acetate. Baseline subtraction, conversion of measured rotations to molar residue ellipticity [θ] (deg cm^2 $dmol^{-1}$), and filtering of the spectra using a FFT filter were performed using the Microcal Origin version 3.5 program.

Fluorescence Anisotropy. Serial dilutions of a concentrated stock of either full-length regulatory subunit homodimer or D/D domain were prepared by diluting the protein with rhodamine-labeled peptide (prepared as described above) in the indicated buffer. For the salt-dependence studies the following buffer was used with varying salt concentrations: 10 mM HEPES pH 7.4, 0−1.2 M NaCl, 3 mM EDTA, 0.005% Surfactant P20 (Biacore). For pH 4.0 and 5.0, the following buffer was used: 10 mM sodium acetate, 150 mM NaCl, 3 mM EDTA, 0.005% Surfactant P20. A peptide concentration of 10 nM was used for RIα and RIIβ isoforms and 1 nM peptide was used for RIIα. The samples were equilibrated for at least 1 h at room temperature with no significant change in anisotropy signal observed for up to 4 h after sample preparation. A Fluoromax-2 (Jobin Yvon Horiba, SPEX Division) equipped with Glan-Thompson polarizers was used to analyze each sample. The alignment of the polarizers was verified using a solution of dextran as the scattering source and found to be within acceptable limits for anisotropy analysis. A circular, quartz cuvette (0.4 cm path length) was used for both RIα and RIIβ. Due to the lower concentration of peptide used for RIIα, a rectangular 1-cm path length quartz cuvette was used to increase the fluorescence signal. The rhodamine-labeled peptide was excited at 541 nm (5−10 nm band-pass) and emission monitored at 575 nm (5−10 nm band-pass). The constant wave analysis (CWA) module of the Fluoromax software was used to take the anisotropy measurements. A 5 s signal integration was used for each orientation of the polarizers, and three separate measurements were averaged, resulting in an anisotropy measurement error of less than two percent. The anisotropy was calculated directly with the Fluoromax software using the following equation:

$$r = (I_{VV} - G^*I_{VH})/(I_{VV} + 2G^*I_{VH}) \quad (1)$$

where r is the steady-state anisotropy, I_{VV} is the fluorescence intensity with the excitation and emission polarizers oriented in the vertical position (0° from normal), I_{VH} is the fluorescence intensity with the excitation polarizer in the vertical position and the emission polarizer oriented in the horizontal position (90°) relative to the excitation polarizer, G is the monochromator grating factor which is equal to (I_{HV}/I_{HH}), with the first subscript indicating the position of the excitation polarizer and the second subscript indicating position of the emission polarizer. G was measured directly for each sample and the average value was 0.601 ± 0.005. Three separate binding experiments were averaged and fit to the following 1:1 binding model using the nonlinear regression application in GraphPad Prism version 3.00 (GraphPad Software):

$$r = (r_{AB} - r_A)X + r_A \quad (2)$$

$$X = \{A_0 + B_0 + K_D - [(A_0 - B_0)^2 + K_D(K_D + 2A_0 + 2B_0)]^{1/2}\}/2A_0 \quad (3)$$

where r is the total anisotropy signal observed, r_{AB} is the anisotropy of the bound species, r_A is the anisotropy of the free peptide, X is the mole fraction of bound species, A_0 is the initial concentration of peptide, B_0 is the initial concentration of protein and K_D is the dissociation constant.

For the competition assays, a saturated complex (100-fold molar excess) of regulatory subunit and rhodamine-labeled peptide was formed (100 nM RII:1 nM peptide and 1000 nM RI:10 nM peptide). A concentrated stock solution of unlabeled RPP8 was serially diluted with either the RII or RI labeled peptide complex solution. The samples were incubated overnight at room temperature and analyzed as described above. The data were fit to a one-site competition model from the nonlinear fit application in GraphPad Prism version 3.00 (GraphPad Software) to obtain the apparent inhibitory constant (appK_I).

GST-Pulldown Assays. Single (E10A, E11A, and D23A) and multiple (E10A−E11A) mutations were made in the GST-RPP8 construct described above using QuikChange (Stratagene) mutagenesis kit. Mutant constructs were expressed in BL21-Gold (DE3) (Stratagene). Bacterial cell lysates containing GST alone, GST-RPP8, GST-RPP8 E10A, GST-RPP8 E11A, GST-RPP8 D23A, and GST-RPP8 E10A−E11A were incubated with glutathione resin (Amersham Biosciences) for 1 h at 4 °C in 10 mM KPO4, 550 mM NaCl, pH 7.4, 0.2% Triton X-100 and washed extensively with the same buffer. RIα or RIIα (35 μM) was added to the immobilized GST constructs and incubated for 1 h at 4 °C. After the resin was washed extensively with buffer, proteins associated with the resin were eluted by boiling in SDS gel loading buffer and analyzed by SDS−PAGE. Proteins were visualized by Coomasie blue staining.

Surface Plasmon Resonance. A BIAcore 3000 was used to measure the kinetics of interaction of the regulatory subunit isoforms binding to RPP8. Each regulatory subunit was immobilized to a cAMP CM5 chip (BIAcore) as previously described (*16*, *20*). Approximately 120 response units (RU) of cAMP was covalently immobilized to the chip using standard amine coupling. Approximately 700 and 1000 RU of RIα and RIIα, respectively, were noncovalently immobilized to the cAMP chip. Serial dilutions of RPP8 were injected over the surface using Kinject at a flow rate of 50 μL/min. Binding was not limited by mass transport at this flow rate. The surface was regenerated using 0.2% SDS followed by a buffer injection. Each kinetic sensorgram was subtracted for bulk solvent effect using a control flow channel which contained only cAMP. The sensorgram was further corrected for channel-specific noise by subtracting a "buffer inject" sample from each sensorgram. Three kinetic experiments using a range of RPP8 concentrations above and below the dissociation constants for each isoform were globally fit to a 1:1 Langemuir interaction model using the BIAevaluation Software (BIAcore) and the following equations:

$$A + B \underset{k_{off}}{\overset{k_{on}}{\leftrightarrow}} AB \tag{4}$$

$$d[AB]/dt = k_{on}[A][B] - k_{off}[AB] \tag{5}$$

where AB is the bound species, A is the analyte concentration (mobile phase), B is the ligand concentration (immobile phase), k_{on} is the association rate constant, and k_{off} is the dissociation rate constant. By substituting in AB = R (response), $B = (R_{max} - R)$ the following equation results:

$$dR/dt = k_{on}A(R_{max} - R) - k_{off}R \tag{6}$$

RESULTS

The Protein Kinase A Binding (AKB) Domain. A 40-residue, C-terminal fragment (R Potential binding Protein, RPP8, Figure 1A) of D-AKAP2 was initially identified in a genomic screen as interacting with the type I regulatory subunit and was subsequently shown to interact with the type II regulatory subunit. The region within RPP8 that was predicted to form a helix and the regulatory subunit binding site corresponded to the first 27 N-terminal residues (RPP8/27, Figure 1A). A helical wheel projection of RPP8/27 revealed an amphipathic helical motif, similar to other AKAPs, beginning with residue 10 and extending to residue 24 (Figure 1B). The repeating hydrophobic, hydrophilic motif results in a helix with defined amphipathicity. We will refer to this motif as the A-kinase binding (AKB) domain. Three acidic residues (E10, E11, and D23) are found within this sequence and are highlighted red. Two of the acidic residues (E10 and D23) bracket both ends of the hydrophobic surface and are highlighted in Figure 1B. The presence of acidic groups in the AKB is not limited to D-AKAP2. Other representative AKAPs contain acidic groups which bracket either the N- or C-terminal of the helical domain and/or are found on the face of the helix opposite the hydrophobic surface (Figure 1C).

pH-Dependent Helix Formation of the AKB Domain. The peptide (RPP8/27) at pH 7.0 is predominantly a random coil as indicated by the far-UV CD spectra (Figure 2A). When the pH is lowered, a characteristic helical spectra is observed with local minima at 208 and 222 nm (Figure 2A). The ellipticity at 222 nm increases (becomes more negative) as a function of decreasing pH and suggests a pH dependence of helix formation (Figure 2B). At pH 3.0, maximal helix formation is observed. This suggests that protonation of aspartic acid and/or glutamic acid side chains, which have pK_a's of 3.9 and 4.2, respectively, may facilitate helix formation.

Regulatory Subunit Binding to the AKB Domain. To characterize the binding affinity of the AKB domain with the regulatory subunit isoforms of PKA, a peptide corresponding to RPP8/27 was synthesized with a C-terminal Cys enabling labeling of the peptide with a fluorescent probe. Steady-state fluorescence anisotropy was used to monitor direct binding of rhodamine-labeled RPP8/27 to the regulatory subunit isoforms. Fluorescence anisotropy measures the mobility of the excited-state fluorophore. Changes in mobility of the fluorophore associated with peptide binding to the regulatory subunit were followed. Binding of RPP8/27 was determined for three of the regulatory subunit isoforms (RIα, RIIα, RIIβ) (Table 1). For both RIα and RIIα, the K_D value of the full-length protein binding to the RPP8/27 was identical to the D/D domain alone, demonstrating that the D/D domain alone was sufficient to form a high-affinity binding site for the D-AKAP2 peptide. The RIIα isoform had the highest affinity for RPP8/27 (K_D = 2.2 nM). This isoform bound 25- and 5-fold more tightly than either the RIα or the RIIβ isoforms, respectively (Table 1). This was

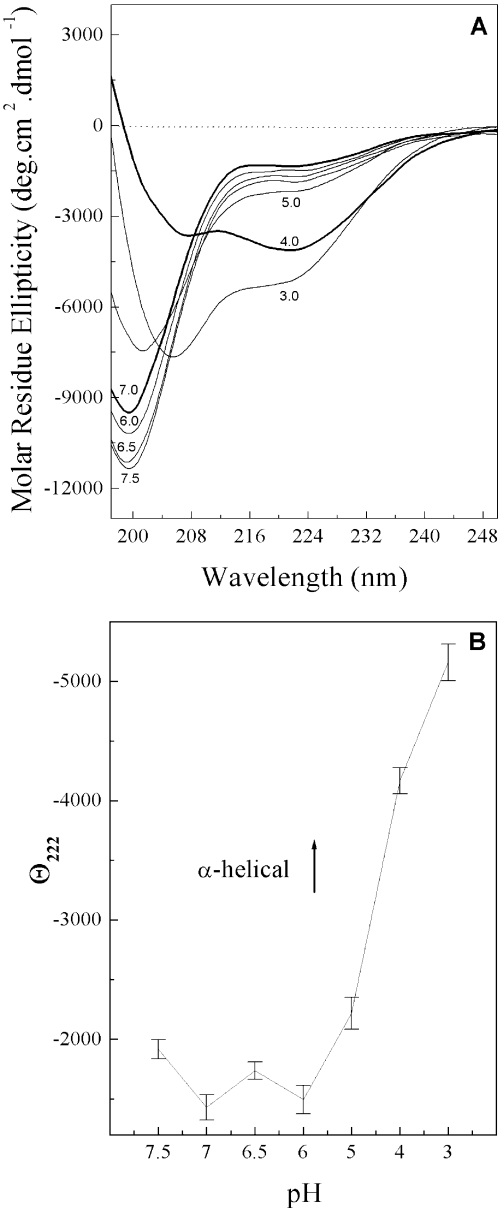

FIGURE 2: The pH-dependence of the secondary structure of the RPP8/27 peptide. (A) Effect of pH on the far-UV CD wavelength spectrum of RPP8/27. pH values used in the titration were 7.5, 7.0, 6.5, 6.0, 5.0, 4.0, and 3.0 and are indicated. (B) Effect of pH on helicity of RPP8/27. The molar ellipticity at 222 nm is plotted versus the pH. Spectra were recorded in either 50 mM sodium acetate or 50 mM sodium phosphate depending on the pH. Peptide concentration was 32 μM. Experiments were performed at 25 °C.

Table 1: Binding Dissociation Constants (K_D) and the Maximal Steady-State Anisotropy (r_{Max}) Values for a Saturated Complex of the Rhodamine-Labeled RPP8/27 Peptide of D-AKAP2 and Each of the Regulatory Subunit Isoforms of PKA

	K_D (nM)	anisotropy (r_{max})
RIα	48 ± 5	0.184 ± 0.002
RIα D/D	52 ± 6	0.131 ± 0.001
RIIα	2.2 ± 0.2	0.194 ± 0.002
RIIα D/D	2.4 ± 0.3	0.144 ± 0.002
RIIβ	13 ± 1	0.208 ± 0.002

not unexpected given the prior knowledge that type II isoforms in general bind more tightly to AKAPs. However, the dissociation constant for the RIα isoform is quite low (K_D = 48 nM) for a dual-specificity AKAP (*20*) and is

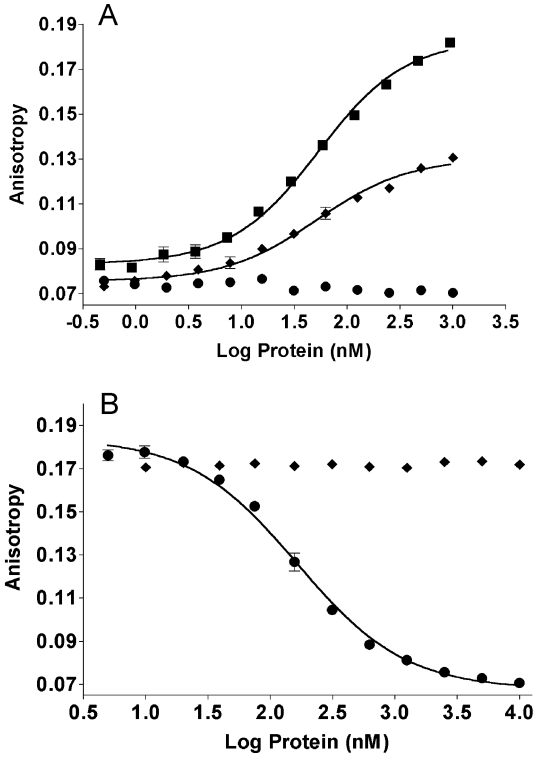

FIGURE 3: (A) Direct binding of full length RIα (■), dimerization/docking (D/D) of RIα (◆) and (Δ1−91) RIα (•) to 10 nM rhodamine-labeled RPP8/27 peptide by steady-state fluorescence anisotropy. No binding was observed with a (Δ1−91) RIα mutant, which lacks the D/D domain. (B) Competition binding assay using a saturated complex of 1 nM rhodamine-labeled RPP8/27 peptide and 100 nM RIIα incubated with increasing concentrations of unlabeled RPP8 (●) or bovine serum albumin (◆). RPP8 effectively competed off the labeled RPP8/27 peptide, whereas the bovine serum albumin had no effect. Experiments were performed in 10 mM Hepes pH 7.4, 150 mM NaCl, 3 mM EDTA, 0.005% Surfactant P20 at 25 °C. K_I values are presented in Table 2.

comparable to that of the RI-specific AKAP, AKAP-CE from *C. elegans* (*21*).

In the unbound state, the peptide had a steady-state anisotropy of 0.075 under the conditions of our fluorescence measurements. Upon binding of the peptide to the regulatory subunit dimer, this value increased in proportion to the amount of peptide bound (Figure 3A). As expected, the fluorescence anisotropy at saturating concentrations of peptide differs significantly between the full-length regulatory subunit dimer and the corresponding D/D domains (Figure 3A and Table 1). The final anisotropy value for the D/D domain was about half that of the full-length protein, reflecting the difference in molecular weight and mobility of the proteins. There was also a 5−10% difference in the anisotropy at saturating peptide concentrations between the peptide bound to RIα versus RIIα and RIIβ subunits. This suggests that the steady-state rotational mobility of the fluorophore when bound to RIIβ is less than when bound to RIα. Although the molecular weights of the regulatory subunits are slightly different (RIα is 87672, RIIα is 90516, and RIIβ is 91982), this anisotropy difference is larger than expected for these molecular weight differences and most likely reflects differences in shape and/or rotational mobility of the different isoforms. This is consistent with small-angle X-ray scattering data, which indicate a significant increase in the radius of gyration (R_g) of RIIβ when compared with

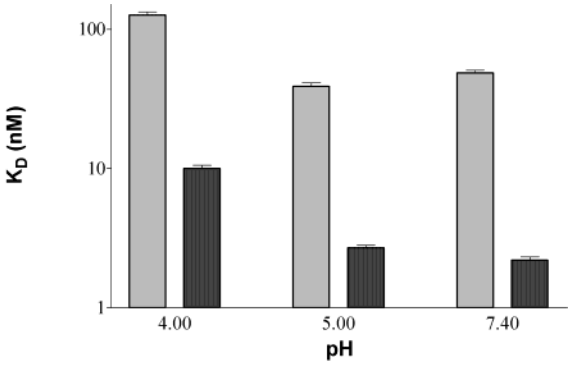

FIGURE 4: The pH-dependence of binding of fluorescently labeled RPP8/27 to both RIα (light gray) and RIIα (dark gray) determined by fluorescense anisotropy. Experiments were performed in 10 mM Hepes, pH 7.4 (sodium acetate for pH 4.0 and pH 5.0), 150 mM NaCl, 3 mM EDTA, 0.005% Surfactant P20 at 25 °C.

RIα (Vigil and Blumenthal, manuscript in preparation). The anisotropy changes observed were specific for AKAP binding, since the type I regulatory subunit which lacks the D/D domain (Δ1−91 RIα) did not induce any anisotropy change in the peptide (Figure 3A).

To determine if the larger RPP8 peptide bound similarly to the various regulatory subunit isoforms, a competition assay was performed. In this assay, a complex was formed with a given isoform and fluorescently labeled RPP8/27. Increasing amounts of unlabeled peptide (RPP8) were added to compete off the labeled peptide (Figure 3B). RPP8 could completely abolish binding of the RPP8/27 peptide to the regulatory subunit (Figure 3B). The competition was specific for RPP8 since a control protein (bovine serum albumin) did not compete off the labeled peptide (Figure 3B). The apparent inhibitory constant (appK_I) for binding of RPP8 to RIIα and RIα was 3.2 ± 0.5 and 114 ± 25, respectively. These were in agreement with the K_D values determined for binding of RPP8/27 to RIIα (Table 1). Therefore, the additional 13 C-terminal residues in RPP8 do not confer any additional affinity to the binding of the D/D domains for either RIα or RIIα.

pH-Dependence of Binding. Given the pH-dependence of α-helix formation of RPP8/27, we decided to evaluate the effects of pH on AKAP binding measured by fluorescent anisotropy. The binding affinities were constant for both the RIα and RIIα isoforms over the pH range 7.4 to 5.0 (Figure 4). However, at pH 4.0, despite the peptide being more helical at this pH, the dissociation constant increased by 2.6- and 4.5-fold for RIα and RIIα, respectively. Therefore, increased helicity did not directly translate into tighter binding, suggesting that acidic residues on the peptide are also important for high affinity interactions with the D/D domain of the regulatory subunits.

Contribution of Acidic Residues. To evaluate the effects of specific acidic residues on binding to the regulatory subunits, the following mutants were constructed in RPP8: E10A, E11A, D23A, and E10A−E11A and tested for their ability to interact with RIα and RIIα using a GST-pulldown assay (Figure 5A,B). The acidic residues are dispensable for binding to RIIα with the mutants and wild-type RPP8 pulling down equivalent amounts of RIIα (Figure 5B). However, binding of RIα was noticeably reduced to D23A, E10A, and

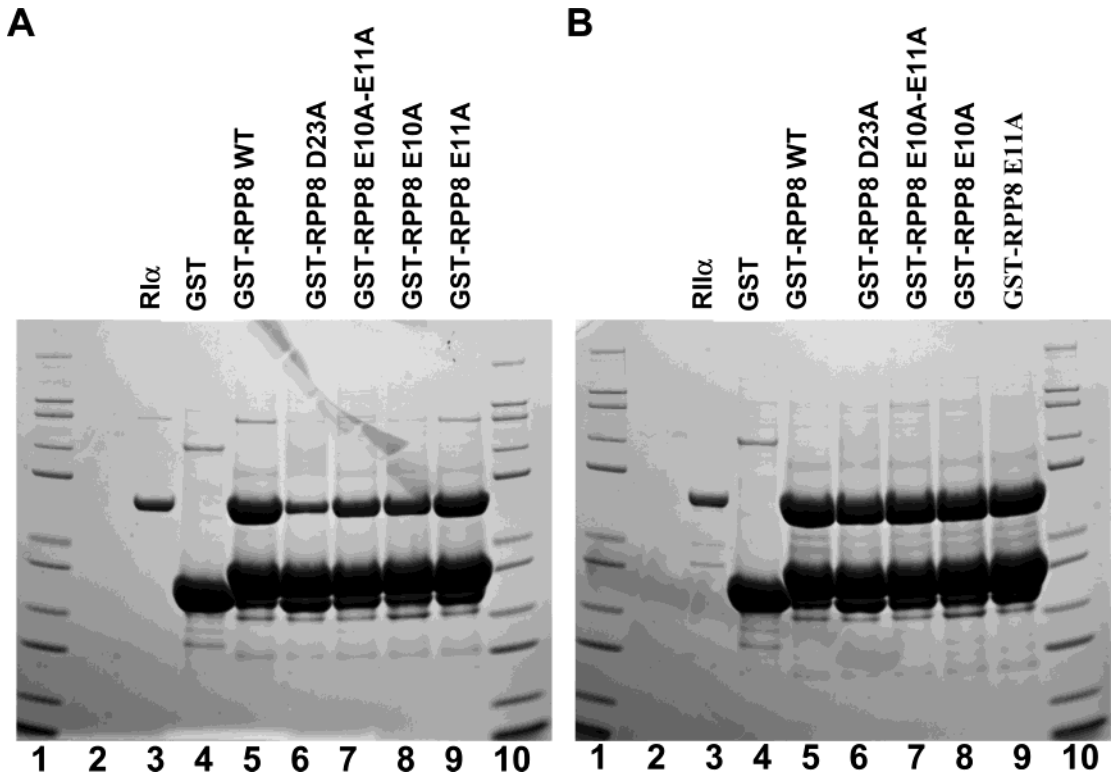

FIGURE 5: Binding of WT and mutant constructs of GST-RPP8 to both RIα (A) and RIIα (B). The GST constructs were immobilized using a glutathione resin and incubated with 35 μM of RIα or RIIα for 1 h at 4 °C. After extensive washing, proteins associated with the GST fused proteins were eluted from the glutathione resin by boiling in SDS gel-loading buffer and analyzed by SDS−PAGE. Lanes 1−10 are as follows for both panels A and B: lane 1, MW marker; lane 2, regulatory subunit (RS) + glutathione resin (control); lane 3, RS standard; lane 4, RS + GST alone (control); lane 5, RS + GST-RPP8 wt; lane 6, RS + GST-RPP8 D23A; lane 7, RS + GST-RPP8 E10A−E11A; lane 8, RS + GST-RPP8 E10A; lane 9, RS + GST-RPP8 E11A; lane 10, MW marker.

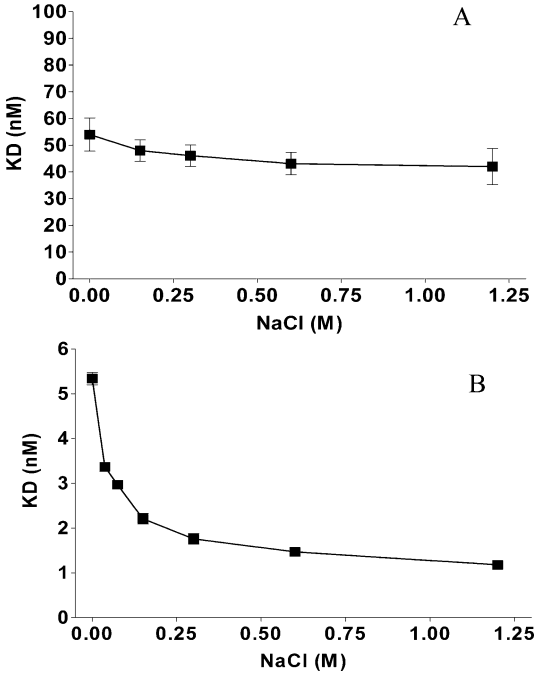

FIGURE 6: The salt-dependence of binding of RPP8/27 peptide with RIα (A) and RIIα (B) determined by fluorescence anisotropy. Experiments were performed with increasing concentrations of NaCl in 10 mM Hepes, pH 7.4, 3 mM EDTA, 0.005% Surfactant P20 at 25 °C.

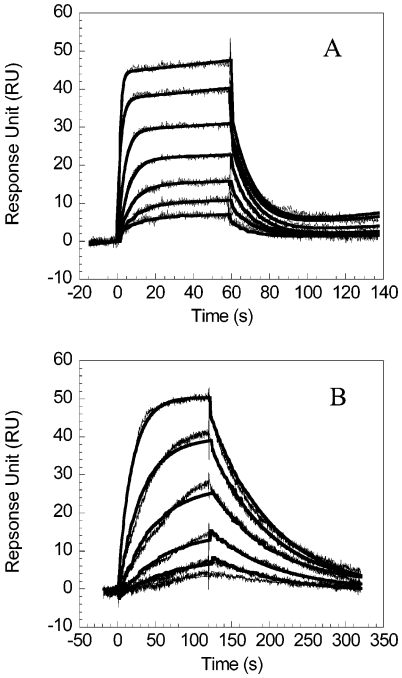

FIGURE 7: Kinetics of interaction of RPP8 with RIα (A) and RIIα (B) using surface plasmon resonance. RIα and RIIα (700 and 1000 RU, respectively) were bound to a cAMP-immobilized CM5 chip. Increasing concentrations of RPP8 were injected over the surface (for RIα 500 nM−5 nM and RIIα 25 nM−0.7 nM) to monitor the on-rate (k_{on}) followed by a buffer inject to monitor the off-rate (k_{off}). The sensorgrams were fit globally to a 1:1 interaction model (solid lines) using BIAevaluation software and the best-fit kinetic parameters summarized in Table 3.

the E10A−E11A double mutant (Figure 5A). This suggested that acidic residues at position E10 at the N-terminus of RPP8 and D23A at the C-terminus and to a lesser extent E11A are important for enhancing the affinity to RIα.

Salt-Dependence of Binding. To evaluate the electrostatic contributions of the interaction suggested by the pH and mutagenesis studies, the salt-dependence of RPP8/27 binding was determined for both isoforms. Binding was evaluated from 0 to 1.2 M NaCl. The dissociation constant for RIα did not change over this broad salt concentration range (Figure 6A). However, RIIα showed a 5-fold decrease in the dissociation constant (increased affinity) at the higher salt concentrations (Figure 6B). This is highly indicative of hydrophobic interactions dominating the binding energy for RIIα:RPP8/27 interactions. If electrostatic interactions were predominating, we would have expected a reduced affinity at higher salt concentrations. The hydrophobic nature of the AKAP:R interaction has been well documented (*2*, *6*). However, the absence of a salt-dependence for RIα binding to D-AKAP2 suggests that a combination of electrostatic and hydrophobic interactions contribute to the RIα binding energy. This is consistent with the mutagenesis studies. Thus, an important difference between RI and RII interactions with D-AKAP2 is the relative importance of electrostatic and hydrophobic interactions.

Binding Kinetics of the AKB to Regulatory Subunit Isoforms. At pH 7.4, the AKB domain from D-AKAP2 binds very tightly to both regulatory subunit isoforms. The unstructured nature of the AKB domain at this pH and the amphipathic nature of the AKB domain sequence suggests that helical formation is induced upon AKAP binding. We have used surface plasmon resonance to evaluate the kinetics of AKB binding to each regulatory subunit isoform. Each regulatory subunit (cAMP free) was bound to the surface of a cAMP-immobilized CM5 chip as described in Materials and Methods and the kinetics of the AKB interaction monitored for each isoform (Figure 7). The observed kinetic data fit well to a 1:1 binding model for both isoforms, suggesting a one-step binding mode of the AKB domain peptide. In addition, the kinetics of interaction were not limited by mass transfer effects, since evaluation over a range of injection flow rates (15−75 μL/min) did not significantly affect the total response (data not shown).

Table 2: Kinetics of Interaction of the D-AKAP2 AKB Domain (RPP8) with RIα and RIIα Isoforms Determined Using Surface Plasmon Resonance[a]

	k_{on} $(M^{-1}\,s^{-1}) \times 10^6$	k_{off} $(s^{-1}) \times 10^{-3}$	K_D (nM)[b]
RIα	1.74 ± 0.07	84.4 ± 5.3	48.6 ± 4.8
RIIα	1.85 ± 0.08	12.2 ± 0.1	6.6 ± 0.3

[a] Kinetic constants were calculated as described in Materials and Methods and represent the mean ± SD of three separate determinations. [b] $K_D = k_{off}/k_{on}$.

The on-rates (k_{on}) for AKB binding did not differ significantly for the two isoforms (Table 2). However, the off-rates (k_{off}) differed by a factor of 7 with the off-rate for the RI interaction being faster than the RII interaction (Table 2). The K_D calculated from the ratio of the on- and off-rates are consistent with the relative affinities determined by the solution-based, fluoresence anisotropy assay.

DISCUSSION

Type I and Type II Isoforms Diversify the cAMP-Mediated Signal. Regulatory subunit isoforms of PKA have evolved to diversify the cAMP-mediated signaling pathway of PKA.

The isoforms differ in their cAMP responsiveness, which directly regulates activation of PKA, and in their ability to bind to AKAPs, which indirectly regulates substrate specificity through PKA localization. Type I isoforms are activated by lower concentrations of cAMP compared with the type II isoforms and bind AKAPs much weaker (*4*, *7*, *22*). The opposing actions of increased cAMP sensitivity and reduced AKAP binding for RI suggest a co-evolution of these regulatory functions controlling the localization and function of the more sensitive type I cAMP trigger.

Dual-specificity AKAPs represent an interesting class of AKAPs because they have the potential to bind both type I and type II regulatory subunit isoforms, thereby recruiting two distinct cAMP responses to a given intracellular location. Although the intracellular functions of the D-AKAPs have remained elusive, several additional D-AKAPs have been identified: D-AKAP1 (*23*), FSC1 domain A (*24*), and PAP7 (*25*). Interestingly, all of the D-AKAPs seem to have in common their association with the mitochondria, suggesting that some aspect of mitochondrial function requires different cAMP responses for PKA holoenzyme activation. The current study has examined the molecular basis for isoform-specific binding of D-AKAP2 to the regulatory subunit isoforms, providing a foundation for understanding the "dual" functionality of this AKAP.

Helix Induction of the AKB and Contribution of Acidic Residues. The PKA binding site (RPP8) at the C-terminus of D-AKAP2 was initially identified in a genomic screen. We have further defined this binding site to a 27-amino acid motif (RPP8/27), which we now refer to as the A-kinase binding (AKB) domain. The AKB domain binds with nanomolar affinity to both RIα and RIIα isoforms of PKA. The high affinity is maintained with the corresponding D/D domain from each isoform, suggesting that this is the essential regulatory subunit domain responsible for binding the dual-specificity AKAP.

We have shown that helix induction of the AKB domain is promoted at low pH in the absence of the D/D domain. This suggests that neutralization of the acidic residues in the AKB domain may be important for inducing the amphipathic helix. By mutating the acidic residues in the AKB domain, we have shown that high affinity binding to RI is dependent on the acidic residues. This is consistent with the lower binding affinity at pH 4.0 in which the acidic residues would presumably be partially protonated. In contrast to RI binding, despite the decreased affinity at low pH for RII binding, acidic residues do not appear to contribute to the binding affinity of RIIα.

Isoform Specific Differences in the Magnitude of the Electrostatic Contribution. The magnitude of the electrostatic contribution to the AKB:R interaction is different for the two isoforms. RIIα shows a clear increase in affinity at higher ionic strength, which is typical of binding reactions that are dominated by hydrophobic contacts. However, binding of the AKB domain to RIα is independent of salt, suggesting that hydrophobic contacts are not the dominating interaction, but rather electrostatics and perhaps hydrogen-bonding play a more prominent role in the AKB:RI interaction. This conclusion is based on the fact that the compensatory action of salt for an interaction that has energetic contributions from both electrostatic and hydrophobic interactions would result in no net change in affinity as salt concentrations are varied over a large range.

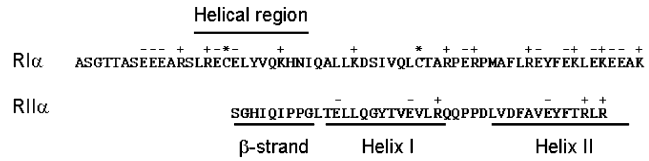

FIGURE 8: Sequence comparison of bovine RIα and murine RIIα dimerization/docking (D/D) domain. Each structure is composed of a similar X-type four helix bundle, which is formed by antiparallel dimerization of each protomer. Helix I forms the AKAP binding surface and helix II forms the majority of the dimerization contacts. The secondary structure differs at the N-terminus with RIα containing an extended helical region and RIIα containing a corresponding β-strand-like region. RIα contains two disulfide bonds covalently linking the isoform-specific helical region with helix I. Basic residues (−) and acidic residues (+) are indicated. The cysteines in RIα are also labeled (*).

Sequence and Structural Differences between RIα and RIIα D/D Domains. The presence of a predominately hydrophobically driven interaction is consistent with the sequence and structural data obtained for the AKB:RII interaction (*2*). The structures of the RIIα D/D domain in the free and AKAP-bound state have been solved by NMR (*6*, *26*). The AKAP is bound to a hydrophobic groove on the surface of the regulatory subunit, dimer interface. This surface shows only minor changes in structure upon binding the AKAP, which suggest a preformed binding surface. Few charged residues surround the hydrophobic groove in RIIα and all of the contact sites were identified as hydrophobic. Although no direct interaction of charged residues with the AKAP were observed in the AKB:RII structure, electrostatic interactions do seem to be important for stabilizing both secondary, tertiary and quaternary structure of the D/D domain (*27*). Since there was no evidence from the mutagenesis studies that acidic residues are playing a direct role in the AKB:RIIα interaction, the decreased binding affinity at the lower pH for RIIα could be the result of an indirect, pH-induced structural effect on the AKAP binding surface of the D/D domain. Alternatively, since we know that at low pH the AKB domain is more helical, changes in helical propensity may also contribute to the reduced binding affinity for RIIα at low pH.

The structure of the RIα D/D has the same overall X-type 4-helix bundle topology, but differs significantly at the N-terminus (*19*). The RIα D/D contains an N-terminal helical segment that partially occludes the AKAP binding surface (Banky, manuscript submitted). This helical segment is restricted by two disulfide bonds at C16 and C37, which covalently cross-link the protomers. Although the disulfides are not required for dimerization (*5*, *18*), they may reduce the conformational freedom of the AKAP:RI interaction, resulting in a more rigid binding surface. In RIIα, the N-terminal segment contains fewer residues and is an extended β-strand-like structure (*26*). Sequence comparison of the extended regions in RIα and RIIα reveal that RIα contains more charged residues in this region (Figure 8) (*19*). These charges presumably reduce the hydrophobic nature of the AKAP binding surface and are consistent with the data presented here in which the acidic residues enhance binding to RI. Therefore, a binding model that includes a combination of both steric and electrostatic differences in the N-terminal extensions of the isoforms could be regulating the AKAP affinity differences observed for these two isoforms. The greater electrostatic component for RIα

binding may contribute to the smaller subset of AKAPs which have been shown to bind RIα since an additional directionality component to AKAP binding could be introduced.

Importance of Acidic Residues in the AKB Domain. Comparison of the AKB domains from many AKAPs has revealed that this motif does not have a strict requirement for particular residues. Instead, a conserved, amphipathic structural motif is required for binding to the regulatory subunit isoforms (Figure 1C). The importance of hydrophobic residues in forming the interaction site with the type II regulatory subunit is well established (*2*). However, the contribution of the charged residues is not well understood. We have shown here that the RI:AKAP interaction has a stronger electrostatic component than the RII:AKAP interaction and that in particular acidic residues have a direct effect on stabilizing the RI:AKAP complex. Whether or not this is a common feature of all RI:AKAP interactions is not clear. AKAPs in general contain varying amounts of charged residues on the surface opposite the hydrophobic surface (Figure 1C). Since there are fewer AKAPs identified that are dual-specific or RI-specific, we are limited in our conclusions regarding conservation of the charged residues. However, several AKAPs whose binding regions have been mapped out (Figure 1C), contain acidic residues either N- or C-terminal to the amphipathic domain. The charges could be important for indirectly stabilizing the helix or for directly interacting with positive charges on the surface of the D/D domain to orient the AKB domain as proposed for the RI:AKAP interaction.

The biological consequences of anchoring different isoforms of PKA to a given intracellular location are still not well understood. We have shown that significant molecular differences do exist between the interactions of the PKA regulatory subunit isoforms and a dual specificity AKAP, D-AKAP2. These differences should be useful in designing isoform-specific disruptors that can be used in vivo to probe the biological effects of isoform-specific anchoring.

ACKNOWLEDGMENT

We would like to thank Dr. Patricia Jennings for her helpful comments during preparation of the manuscript, Dr. Yoshitomo Hamuro for his contribution in deriving the steady-state binding equation used to quantitate the protein−peptide interaction, Simon Brown and Ben Boe for their help in purifying proteins, and Siv Garrod for purifying the D-AKAP2 peptide.

REFERENCES

1. Taylor, S. S., Buechler, J. A., and Yonemoto, W. (1990) cAMP-dependent protein kinase: framework for a diverse family of regulatory enzymes. *Annu. Rev. Biochem. 59*, 971−1005.
2. Colledge, M., and Scott, J. D. (1999) AKAPs: from structure to function. *Trends Cell Biol. 9*, 216−21.
3. Edwards, A. S., and Scott, J. D. (2000) A-kinase anchoring proteins: protein kinase A and beyond. *Curr. Opin. Cell Biol. 12*, 217−21.
4. Skalhegg, B. S., and Tasken, K. (2000) Specificity in the cAMP/PKA signaling pathway. Differential expression,regulation, and subcellular localization of subunits of PKA. *Front. Biosci. 5*, D678−93.
5. Banky, P., Huang, L. J., and Taylor, S. S. (1998) Dimerization/docking domain of the type Ialpha regulatory subunit of cAMP-dependent protein kinase. Requirements for dimerization and docking are distinct but overlapping. *J. Biol. Chem. 273*, 35048−55.
6. Newlon, M. G., Roy, M., Morikis, D., Carr, D. W., Westphal, R., Scott, J. D., and Jennings, P. A. (2001) A novel mechanism of PKA anchoring revealed by solution structures of anchoring complexes. *EMBO J. 20*, 1651−62.
7. Feliciello, A., Gottesman, M. E., and Avvedimento, E. V. (2001) The biological functions of A-kinase anchor proteins. *J. Mol. Biol. 308*, 99−114.
8. Barradeau, S., Imaizumi_Scherrer, T., Weiss, M. C., and Faust, D. M. (2001) Muscle-regulated expression and determinants for neuromuscular junctional localization of the mouse RIalpha regulatory subunit of cAMP-dependent protein kinase. *Proc. Natl. Acad. Sci. U.S.A. 98*, 5037−42.
9. Imaizumi-Scherrer, T., Faust, D. M., Barradeau, S., Hellio, R., and Weiss, M. C. (2001) Type I protein kinase a is localized to interphase microtubules and strongly associated with the mitotic spindle. *Exp. Cell. Res. 264*, 250−65.
10. Skalhegg, B. S., Tasken, K., Hansson, V., Huitfeldt, H. S., Jahnsen, T., and Lea, T. (1994) Location of cAMP-dependent protein kinase type I with the TCR−CD3 complex. *Science 263*, 84−7.
11. Brandon, E. P., Idzerda, R. L., and McKnight, G. S. (1995) Knockouts. Targeting the mouse genome: a compendium of knockouts (Part I). *Curr. Biol. 5*, 625−34.
12. Amieux, P. S., Cummings, D. E., Motamed, K., Brandon, E. P., Wailes, L. A., Le, K., Idzerda, R. L., and McKnight, G. S. (1997) Compensatory regulation of RIalpha protein levels in protein kinase A mutant mice. *J. Biol. Chem. 272*, 3993−8.
13. Cummings, D. E., Brandon, E. P., Planas, J. V., Motamed, K., Idzerda, R. L., and McKnight, G. S. (1996) Genetically lean mice result from targeted disruption of the RII beta subunit of protein kinase A. *Nature 382*, 622−6.
14. Amieux, P. S., Howe, D. G., Knickerbocker, H., Lee, D. C., Su, T., Laslo, G. S., Idzerda, R. L., and McKnight, G. S. (2002) Increased basal PKA activity inhibits the formation of Mesoderm-derived structures in the developing mouse embryo. *J. Biol. Chem. 277*, 27294−304.
15. Huang, L. J., Durick, K., Weiner, J. A., Chun, J., and Taylor, S. S. (1997) D-AKAP2, a novel protein kinase A anchoring protein with a putative RGS domain. *Proc. Natl. Acad. Sci. U.S.A. 94*, 11184−9.
16. Hamuro, Y., Burns, L. L., Canaves, J. M., Hoffman, R. C., Taylor, S. S., and Woods, V. J. (2002) Domain organization of D-AKAP2 revealed by enhanced deuterium exchange-mass spectrometry (DXMS). *J. Mol. Biol. 321*, 703−14.
17. Pace, C. N., Vajdos, F., Fee, L., Grimsley, G., and Gray, T. (1995) How to measure and predict the molar absorption coefficient of a protein. *Protein Sci. 4*, 2411−23.
18. Leon, D. A., Herberg, F. W., Banky, P., and Taylor, S. S. (1997) A stable alpha-helical domain at the N terminus of the RIalpha subunits of cAMP-dependent protein kinase is a novel dimerization/docking motif. *J. Biol. Chem. 272*, 28431−7.
19. Banky, P., Newlon, M. G., Roy, M., Garrod, S., Taylor, S. S., and Jennings, P. A. (2000) Isoform-specific differences between the type I alpha and type II alpha cyclic AMP-dependent protein kinase A anchoring domains revealed by solution NMR. *J. Biol. Chem. 275*, 35146−35152.
20. Herberg, F. W., Maleszka, A., Eide, T., Vossebein, L., and Tasken, K. (2000) Analysis of A-kinase anchoring protein (AKAP) interaction with protein kinase A (PKA) regulatory subunits: PKA isoform specificity in AKAP binding. *J. Mol. Biol. 298*, 329−39.
21. Angelo, R., and Rubin, C. S. (1998) Molecular characterization of an anchor protein (AKAPCE) that binds the RI subunit (RCE) of type I protein kinase A from *Caenorhabditis elegans*. *J. Biol. Chem. 273*, 14633−43.
22. Doskeland, S. O., Maronde, E., and Gjertsen, B. T. (1993) The genetic subtypes of cAMP-dependent protein kinase−functionally different or redundant? *Biochim. Biophys. Acta 1178*, 249−58.
23. Huang, L. J., Durick, K., Weiner, J. A., Chun, J., and Taylor, S. S. (1997) Identification of a novel protein kinase A anchoring protein that binds both type I and type II regulatory subunits. *J. Biol. Chem. 272*, 8057−64.
24. Miki, K., and Eddy, E. M. (1998) Identification of tethering domains for protein kinase A type Ialpha regulatory subunits on sperm fibrous sheath protein FSC1. *J. Biol. Chem. 273*, 34384−90.
25. Li, H., Degenhardt, B., Tobin, D., Yao, Z. X., Tasken, K., and Papadopoulos, V. (2001) Identification, localization, and function

in steroidogenesis of PAP7: a peripheral-type benzodiazepine receptor- and PKA (RIalpha)-associated protein. *Mol. Endocrinol. 15*, 2211−28.

26. Newlon, M. G., Roy, M., Morikis, D., Hausken, Z. E., Coghlan, V., Scott, J. D., and Jennings, P. A. (1999) The molecular basis for protein kinase A anchoring revealed by solution NMR. *Nat. Struct. Biol. 6*, 222−7.
27. Morikis, D., Roy, M., Newlon, M. G., Scott, J. D., and Jennings, P. A. (2002) Electrostatic properties of the structure of the docking and dimerization domain of protein kinase A IIalpha. *Eur. J. Biochem. 269*, 2040−51.

BI0265729